Mon. Not. R. Astron. Soc. **000**, 000–000 (2001)

Dynamical evolution of rotating stellar systems – II. Post-collapse, equal mass system

E. Kim[1,2], C. Einsel[2], H.M. Lee[1,3], R. Spurzem[2], and M.G. Lee[1]
[1] *Astronomy Program, SEES, Seoul Nat. Univ., Seoul 151-742, Korea*
[2] *Astronomisches Rechen-Institut, Mönchhofstrasse 12-14, 69120 Heidelberg, Germany*
[3] *Institute of Space and Astronautical Science, Sagamihara, Japan*

7 September 2001

ABSTRACT

We present the first post core collapse models of initially rotating star clusters, using the numerical solution of an orbit-averaged 2D Fokker-Planck equation. Based on the code developed by Einsel & Spurzem (1999), we have improved the speed and the stability and included the steady three-body binary heating source. We have confirmed that rotating clusters, whether they are in a tidal field or not, evolve significantly faster than non-rotating ones. Consequences for observed shapes, density distribution, and kinematic properties of young and old star clusters are discussed. The results are compared with gaseous and 1D Fokker-Planck models in the non-rotating case.

Key words: gravitation – methods: numerical – celestial mechanics, stellar dynamics – globular clusters: general

1 INTRODUCTION

Dynamical modeling of globular clusters and other collisional stellar systems (like galactic nuclei, rich open clusters, rich galaxy clusters) still suffers from severe drawbacks. They are due partly to the poor understanding of the validity of assumptions used in statistical modeling based on the Fokker-Planck and other approximations on one hand, and due to statistical noise and the impossibility to directly model realistic particle numbers with the presently available hardware, on the other hand. For rich star clusters with 10^5 or more particles this statement is still true, despite of continuous progress in the development and application of special purpose computers (cf. e.g. Makino & Hut 2001).

Therefore a detailed comparison of the different methods is very important using the same choices of parameters and initial data. For spherical, non-rotating star clusters this has been provided in the last decade (Giersz & Heggie 1994a,b, henceforth GHI, GHII, Giersz & Spurzem 1994, henceforth GS, Spurzem & Aarseth 1996, Spurzem 1996). The basic idea of such comparisons is to check the validity of models based on statistical mechanics, e.g. by using the Fokker-Planck approximation, against direct orbit integration of large N-body systems using state-of-the art direct N-body codes. Depending on the model a number of free parameters (such as a free factor in the argument of the Coulomb logarithm, to mention one typical example) can be adjusted. Since the number of free parameters, however, is small, a positive result in the comparison for many values of N (particle number) and different initial models is considered as a proof of the underlying physical concepts and approximations. Such systematic comparisons even across a larger number of participating groups have a tradition in the field of collisional N-body and star cluster modelling (Lecar & Cruz-González 1972, Heggie et al. 1998) and will be continued in the future (Heggie 2001).

On the side of theoretical or statistical mechanics we mainly use the Fokker-Planck equation and the direct numerical solution of its orbit average. One example is 1D models (assuming that the distribution function f only depends on a single constant of motion, the energy E of a stellar orbit in the given spherical potential), applicable for isotropic spherical systems (Cohn 1980). There are generalizations to 2D anisotropic models, where f depends on two independent variables, energy and angular momentum J^2 (Cohn 1979, Takahashi 1995, 1996, 1997, Takahashi, Lee & Inagaki 1997), thus including the possible difference between radial and tangential velocity dispersions in a cluster and (in the last cited paper) the effect of a tidal boundary. For recent models including tidal fields and a stellar mass spectrum compare e.g. Takahashi & Lee (2000) and Takahashi & Portegies Zwart (1998, 2000). Another type of statistical models is so-called gaseous models, which solve numerically, similar to solutions of gas dynamical equations, a set of moment equations of the Fokker-Planck equation. They are usually taken up to second order and terminated by a heat flux equation in third order (Heggie 1984), including as well the anisotropy (Louis & Spurzem 1991, Spurzem 1994).

On the other side there are direct N-body models using standard N-body codes (NBODY5: Aarseth 1985, Spurzem & Aarseth 1996; NBODY4: Makino & Aarseth 1992, Makino 1996, Aarseth & Heggie 1998, NBODY6 and NBODY6++: Aarseth 1996, 1999a, Spurzem 1999, Spurzem & Baumgardt 2001) or Monte Carlo schemes (Giersz 1996, 1998, 2001, Joshi, Rasio & Portegies Zwart 2000, Joshi, Nave & Rasio 2001). The Monte Carlo models, being comparable in their wealth of data and stochastic nature to the direct N-body models, still employ the Fokker-Planck approximation.

Orbit-averaged Fokker-Planck and direct N-body models in particular have been improved sometimes by including very detailed astrophysical ingredients, such as a stellar mass spectrum (Spurzem & Takahashi 1995, Giersz & Heggie 1997, Heggie et al. 1998), adding to that a more detailed treatment of the tidal truncation (Takahashi, Lee & Inagaki 1997), or approximate modelling of gravitational shocking (Gnedin, Lee & Ostriker 1999), or very detailed treatments of single and binary stellar evolution, coupled with a detailed follow-up of merging and collisions (Portegies Zwart et al. 1999, Hurley et al. 2001). The cited papers are just recent examples and not exhaustive; the interested reader could get a better overview e.g. by looking at the proceedings volume of Deiters et al. (2001). The comparison of different ways of modelling, though not as exhaustive yet as in the idealized single mass case, has been done at least by studying some selected problems regarding tidal mass loss in direct Fokker-Planck versus N-body models (Portegies Zwart & Takahashi 1999, Takahashi & Portegies Zwart 1998, Baumgardt 2001).

The results could be summarized by saying that in general the Fokker-Planck approximation (small angle two-body scattering dominates the global evolution of the system), the approximation of heat conduction (its energy transport can be treated as heat conduction in a collisional gas), and the statistical binary treatment (model of energy generation by formation and subsequent hardening of three-body binaries using simple semi-analytical estimates) all appear to be a fairly good description of what happens in N-body simulations. But there are still two basic drawbacks:

(i) all comparisons are so far limited to rather small particle numbers ($N \leq 64000$) as compared to real particle numbers of globular clusters of the order of a few 10^5 or even up to 10^6 stars. Low N models cannot be easily extrapolated to higher N, since after core collapse a variety of different processes (close encounters, tidal two-body encounters, effects of the finite size of the stars) all vary with time scales, which depend on different powers of the particle number (see e.g. the scaling problem tackled by Aarseth & Heggie 1998);

(ii) during core bounce and binary driven post-collapse evolution an individual N-body simulation exhibits stochastic fluctuations, due to the stochastic occurrence of superelastic scatterings of very hard binaries with field stars and other binaries. Although the averaged evolution of the system, understood either as a time average (looking for long post-collapse times) or as an ensemble average (averaging statistically independent single N-body models), is reproduced well by the theoretical models based on the above assumptions, the *individual* evolution of a stellar system, even with a relatively large particle number, might not be exactly matched at any instant. The collaborative experiment in this area (Heggie et al. 1998) gives a good overview: all methods do agree fairly well, but variations of quantitative results of some 10 or 20 % and some scaling problems, which are not exhaustively examined, have to be tolerated.

Very few attempts yet have been done to include a rather important piece of realism, the existence of an initial angular momentum of the star cluster. While the probability that the cloud from which a star cluster originates, has zero total angular momentum is very small, practically all models have assumed that. The inclusion of angular momentum requires a much more complex physical treatment, including axisymmetry in coordinate space (flattened clusters) and a way to deal with a third integral of motion of individual stellar orbits, which is not known analytically in general.

First semi-analytical models by Agekian (1958) assumed that escaping stars have the same angular momentum distribution with the remaining ones, and the system keeps a structure as a MacLaurin spheroid. In particular the first approximation is rather doubtful, as one could already deduce from an unpublished early direct Fokker-Planck model by Goodman (1983). Goodman's work was revisited and improved by a much more detailed numerical 2D Fokker-Planck study of core collapse of rotating star clusters by Einsel & Spurzem (1999, henceforth Paper I, see also Spurzem 2001). In a slightly different approach Hachisu (1979) argued that there would be an internal, relaxation driven redistribution of angular momentum, similar to the mechanism of gravothermal collapse. In Paper I it was found that such internal redistribution occurs in the early evolutionary phase, but later mass loss and relaxation due to angular momentum loss connected with it dominates the evolution. Also it was found there (by inspection of the numerical results), that in the late stages of core collapse a self-similar solutions exists in which the rotational velocity scales with the same power as the velocity dispersion; this finding was underlined by some theoretical arguments of Lynden-Bell (2001).

Paper I demonstrated, that the influence of rotation on star cluster evolution is not small. The core collapse time could be accelerated very much (that was an equal mass model). So, it is not clear, what is the combined influence of rotation and the other processes, which had been improved and included into cluster dynamics in the past (stellar evolution, mass spectrum, tidal fields and tidal shocking, primordial binaries).

Unfortunately, rotation, though it is a natural initial condition from collapse of a star–forming cloud, could not be included in most of the existing evolutionary models of star clusters. Monte Carlo and Fokker-Planck techniques (with the exception of Paper I) were limited to spherical symmetry, as well as gaseous models. A generalization of such models poses significant challenges, such as what is the effective viscosity scaling describing properly viscous effects due to two-body relaxation (Goodman 1983) in the case of gaseous models. For Fokker–Planck models the main problem is the requirement to neglect a possibly existing third integral of motion on axisymmetric potentials, because it cannot be given analytically. In Paper I diffusion of orbits was considered disregarding the third integral, i.e. in a 2D model only considering E and J_z, orbital energy and z-component of angular momentum of a stellar orbit, and a discussion of possible errors was given.

In this paper we continue and improve the work of Paper I in several respects. First we include a statistical binary

energy generation, to model the heating of the core of the cluster in late stages of core collapse due to the formation and subsequent superelastic scatterings of hard binaries in three-body encounters (Hut 1985, Lee, Fahlman & Richer 1991). So, the evolution of the cluster, its shape and internal parameters, such as density distribution, rotation curve, velocity dispersions and mass loss in a steady tidal field, will be followed past the time of maximum collapse, where the models of Paper I stopped. These are the first post-collapse Fokker-Planck models of rotating star clusters published so far.

Furthermore, we have improved the quality of the numerical integration scheme to have a better ground for comparisons with other methods, and an attempt has been made to disentangle the effects of rotation and tidal cutoff, which was not clear in Paper I, by comparing isolated models (spatially extrapolated models to infinity without energy cutoff, but otherwise following the density structures of our King models) with the tidally truncated ones. In future work N-body models will be provided for comparisons as well. Some preliminary results can be obtained from Boily (2000) and Boily & Spurzem (2000). They show that for moderate amounts of rotation the Fokker-Planck and N-body models agree rather well. Also, we compare in the non-rotating case the results of our code with standard models (1D Fokker Planck codes by H.M. Lee and K. Takahashi, gaseous model by R. Spurzem).

It should be noted that our models are still on a rather idealized level: there is no stellar mass spectrum, no effects of finite size stars, no time dependent tidal field, no primordial binaries. However, we stress the importance to study first the undisturbed physical effect of rotation on the standard picture of star cluster evolution. Since rotation is such a fundamental initial and natural physical parameter, this is considered as a per se interesting study of dynamics of N-body systems, but it has also strong astrophysical relevance, because the characteristics of rotation may be a parameter which is less severely influenced than others by core collapse and post collapse re-expansion, at least around the half-mass radius. So it is a possible diagnostic tool to determine dynamical ages of clusters and to set constraints on the cluster's initial configurations. Also, galactic nuclei containing supermassive black holes are mostly rotating systems, and the physical and numerical techniques developed here find their application also for a consistent time-dependent modeling of galactic nuclei.

This paper is organized as follows. In the next section, we briefly describe our models. In §3, we present the results of the post-collapse cluster evolution of initially rotating clusters, and discuss the implications of our results. The conclusion is given in the last section.

2 THE MODELS

2.1 Numerical Method

A computational scheme to solve the 2D Fokker-Planck (henceforth FP) equation with high accuracy for pre- and post-collapse has been worked out. The framework of the method is the same as that of Paper I: it is comprised of two steps, one is the FP step, in which the distribution function is advanced by solving the FP equation with the gravitational potential being held fixed. In the Poisson step, the potential is advanced by solving Poisson's equation with the distribution function being held fixed as a function of the adiabatic invariants. Henceforth, the code developed to study dynamical star cluster with 2D Fokker-Planck equation is called FOPAX.

In the following we describe some improvements from previous works. First we have improved the Poisson step, on which the global accuracy of the computation depends very much, as noted in Paper I. We have changed a part where the volume of the hypersurface for given energy and angular momentum and the adiabatic invariant are calculated (see eqs. (5) & (7) in Paper I). In the previous version of code these quantities are calculated by using simple trapezoidal rule. Now we use a two dimensional Gaussian quadrature scheme. A comparison of the adiabatic invariants calculated by using these two different schemes showed that stars with nearly circular orbits around the cluster center are more accurately computed with the new scheme. We note also, that the diffusion coefficients become more accurate than the previous code thanks to the improved accuracy in computing the volume of the hypersurfaces.

As for the FP step, an essential difference between the method used here and that in Cohn (1979) is concerning the discretization: we apply a finite difference scheme, where the Chang-Cooper scheme is applied only for the energy direction (compare also for the anisotropic spherical 2D case by Takahashi 1995).

In order to extend the evolution beyond the core collapse, we need to add an energy source that drives the post core collapse evolution. Primordial binaries and massive stars can provide energy from very early on, and they delay significantly the core collapse time and affect the details of the binary distribution very much (Gao et al. 1991, Giersz & Spurzem 2000). In order to compare well our models with previous standard results, and due to a lack of any good method to include many hard binaries in our model, we have only considered the heating effect due to three-body binaries.

The energy generation rate by three-body binaries per mass unit is given as (e.g., Hut 1985)

$$\left(\frac{\delta e}{\delta t}\right)_{\rm 3b} = C_b \frac{\rho^2}{m^2\sigma^2}\left(\frac{Gm}{\sigma}\right)^5 \quad . \tag{1}$$

Here ρ and σ are the local mass density and 1D velocity dispersion, respectively, G the gravitational constant and m the individual stellar mass. It is shown in Giersz & Spurzem (1994) and Giersz & Heggie (1994a,b) that for particle numbers between $N = 1000$ and $N = 10000$ the best agreement between direct N-body calculations, direct solutions of the orbit-averaged Fokker-Planck equation and anisotropic gaseous models is achieved for one set of parameters, including the parameter of the Coulomb logarithm $\gamma = 0.11$, and $C_b = 90$. The latter value used to be the standard value derived from theoretical arguments, based on a numerical factor of $\tilde{C} = 0.9$ in the formula for the formation rate of three-body binaries (Hut 1985). It has been argued (Goodman & Hut 1993), that $\tilde{C} = 0.75$ is a better choice, but still within some uncertainty. The results of comparisons with N-body simulations show that $C_b = 90$ is a fairly reasonable value, but within the uncertainty $C_b = 75$ (which would

Table 1. Properties of Initial Models

W_0	ω_0	r_t/r_c	r_h/r_t	$T_{rot}/\|W\|$	e_{dyn}	r_h [pc]	τ_{rh} [yrs]
6	0.0	18.0	0.15	0.000	0.000	4.19	1.64×10^8
	0.3	14.5	0.18	0.035	0.107	5.02	2.15×10^8
	0.6	9.6	0.24	0.101	0.285	6.70	3.32×10^8
3	0.0	4.7	0.26	0.000	0.000	7.25	3.73×10^8
	0.8	4.2	0.29	0.035	0.102	8.89	4.40×10^8
	1.5	3.3	0.35	0.097	0.267	9.77	5.84×10^8

e_{dyn}: dynamical ellipticity as defined in Paper I.
$T_{rot}/|W|$: rotational over potential energy.
$m = 1M_\odot$ assumed to compute dimensional quantities. We have used fixed value of $r_t = 27.9$ pc to obtain r_h.

ensue with the new formation rate) cannot be ruled out. However, we also note that the detailed evolution is very insensitive to this constant.

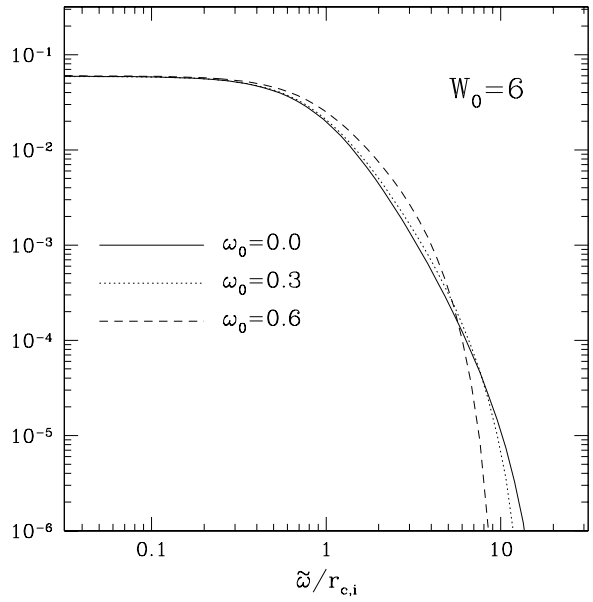

Figure 1. The density profiles along the major axis of selected initial models. Rapidly rotating model is less centrally concentrated than slowly rotating or non-rotating model.

2.2 Initial Models and Boundary Conditions

As in Paper I, we employ the rotating King models as initial models following Lupton & Gunn(1987). These models are characterized by two parameters: dimensionless central potential W_0 and the rotational parameter ω_0. We have examined the evolution of clusters with $W_0 = 6$ and W_0=3. The rotational parameters are chosen such that the cluster remains to be stable against the dynamical instabilities. In Table 1, we have listed the global parameters of the initial models used in the present study. The rotation parameters for models with central potential $W_0 = 3$ are chosen such that the ratios of initial rotational energy to initial potential energy should be similar to those for models with central potential $W_0 = 6$ as shown in Table 1. For uniformly rotating systems, secular instability is known to arise if $T_{rot}/|W| > 0.14$ (Ostriker & Peebles, 1973), where T_{rot} is the rotational kinetic energy and W is the potential energy. All of our models satisfy the stability criterion.

The density structures along major axis of the initial models for $W_0 = 6$ and $\omega_0 = 0$, 0.3 and 0.6 are shown in Fig. 1. The density profiles are similar to each other except near the tidal boundary. As we have seen from Table 1, the r_t/r_c becomes smaller as ω_0 increases. Therefore, the rapidly rotating clusters are less centrally concentrated than slowly rotating or non-rotating clusters with the same W_0.

We have considered two different boundary conditions: tidally limited and isolated cases. For the tidally limited models, we assumed that the cluster orbits in the spherical potential of its mother galaxy at a constant distance (circular orbit), so that the mean density within the tidal radius (r_t) remains a constant throughout the evolution. We have removed stars beyond the tidal radius instantaneously at every Poisson step. This boundary condition is clearly somewhat extreme. In actual clusters, the stars remain near the tidal boundary for orbital time scales. Depending on the treatment of the evaporation process, the lifetime of the clusters could vary significantly, especially for small N clusters (Takahashi & Portegies Zwart 2000). As we will specify later, our models actually use rather small N in order to reduce the computing time (see below). By using small N, the core collapse stops at relatively small core density. However, the outer parts are not sensitive to the choice of N, except for evaporation times (in units of half-mass relaxation time). We can interpret our results as those of large N for the long-term evolution of the global properties.

For the case of the isolated models, we have to extend the calculation to infinite distance which is impossible. Thus we set the computational boundary at $10\,r_{t,i}$, where $r_{t,i}$ is the tidal radius of the initial model. If the stars reach beyond this radius, they are 'removed'. The mass lost by this process is usually very small. A similar boundary condition was used in computing the evolution of isolated clusters in previous studies (see, for example, Quinlan 1996). We found that very little mass is lost for isolated clusters until the end of computation with this boundary condition. Therefore we can study the influence of rotation on relaxation alone, without interference of the (tidal) mass loss processes.

The pre-collapse evolution does not depend on the total number of stars (N). However, the relative importance of the binary heating to the two-body relaxation depends on N. Larger N means higher central density at the time of expansion, and thus longer computational time. If N is too small, we cannot apply the Fokker-Planck method. As a compromise, we have used $N = 5000$ for the models considered in the present paper. This is obviously much smaller than that of actual globular clusters, and brings relaxation time and crossing time closer to each other than in real clusters. According to recent comparisons between direct FP and N-body models (Takahashi & Portegies Zwart 1998, Portegies Zwart & Takahashi 1999) the evolution of the total mass of the cluster until total dissolution depends rather sensitively on the particle number, because the mass loss process

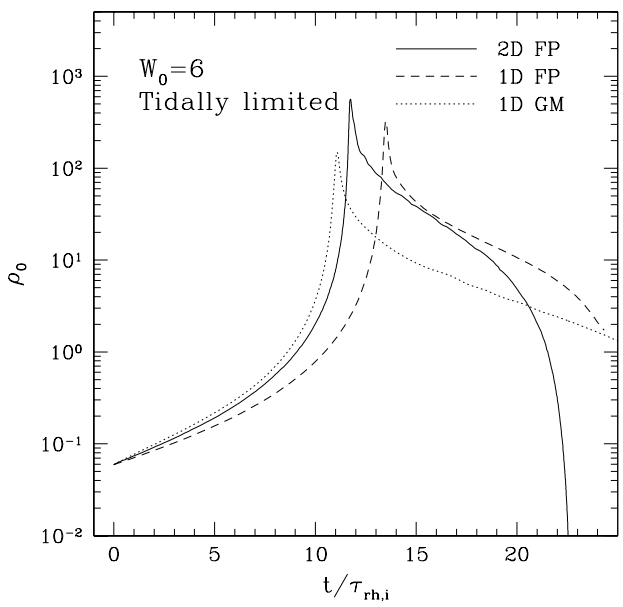

Figure 2. Comparison of central density evolution for model with $(W_0 = 6, \omega_0 = 0)$ between FOPAX (solid line), 1D FP (dashed line) and 1D gaseous model (dotted line).

involves the crossing time rather than the relaxation time. Nevertheless we restrict ourselves here to models using relatively small N, because this speeds up the computation (not so deep central collapse is reached) and we mainly want to study here the interplay between rotation, relaxation and tidal mass loss, where it is an advantage to have the relevant time scales not too different from each other. Also, $N = 5000$ is already large enough to study the effect of core bounce caused by formation and hardening of three-body binaries. A more detailed and realistic modelling should include more cluster physics anyway, so we do not provide models with large N here, but restrict ourselves to this rather theoretical study of relaxing rotating collisional star clusters.

3 RESULTS AND DISCUSSIONS

3.1 Non-rotating Limit

First, we compare the evolution of tidally limited clusters by FOPAX (assuming $\omega_0 = 0$), 1D FP and gaseous models. The evolution of central density of tidally limited, non-rotating models with the central King potential of $W_0 = 6$ is shown in Fig. 2. The results obtained by the 1D FP code (Lee, Fahlman & Richer 1991) and 1D gas model (e.g., Spurzem 1996), are shown as broken and dotted lines, respectively. The time is expressed in units of initial half-mass relaxation time ($\tau_{rh,i}$), and the central density in units of $M_i/r_{c,i}^3$, where M_i and $r_{c,i}$ are initial mass and King's core radius, respectively.

There are some differences in collapse times among different methods. 1D Fokker-Planck model has the longest and the gaseous model has the shortest collapse times. Quinlan (1996) reported that the isotropic 1D model with initial $W_0 = 6$ reaches the core-collapse at 12.94 $t_{rh,0}$, which is about 6% shorter than our 1D model shown in Fig. 2. Part of the difference is due to the binary heating: when the binary heating is turned off, the core collapse time becomes around 13.4 $t_{rh,0}$, which is about 3.5% longer than Quinlan (1996), but in perfect agreement with another type of calculations by K. Takahashi (private communication) using the anisotropic Fokker-Planck code in (E, J) where development of anisotropy is suppressed.

The FOPAX, applied to an initially non-rotating cluster reaches the core collapse in shorter time than any of the other isotropic 1D models. The central density for 2D FP model at the time of core collapse is larger by a factor ~ 2 than that of 1D FP model. In principle, these calculations should give the same result, but because of different treatment of the detailed numerical integration, we regard these discrepancies as insignificant for the general behavior of the long term evolution. The lifetime of the rotating 2D Fokker-Planck model is also shorter by about 10 % than isotropic model.

The collapse time for 1D gas model is shorter than other computations by about $5 \sim 20\%$. The difference of collapse time between gas model and FP model is also seen elsewhere (Spurzem & Takahashi 2001), where it is interpreted as a result of different physical approximations used in gas and Fokker-Planck models.

3.2 Isolated and Tidally Limited Models

Fig. 3 displays the time evolution of central density for our 9 models. Solid lines represent the run of central density with tidal boundary and dashed lines for isolated cases. The acceleration of core collapse due to rotation is shown clearly for both types of boundary conditions. The tidally limited rotating models reach core collapse earlier than non-rotating ones, when the time is measured in units of half-mass relaxation time $\tau_{rh,i}$, as reported in Paper I. However, the evolution of central density of isolated stellar systems was not computed previously. The acceleration of core collapse owing to initial rotation for an isolated stellar system is clearly visible in Fig. 3a. However, the acceleration of core collapse in a rotating star cluster (as compared to the non-rotating models) is stronger if also tidal mass loss is present (which was the case only studied in Paper I). So we have distinguished the two major effects accelerating core collapse in rotating star clusters, one is due to enhanced two-body relaxation alone, and the other is a coupling of rotation with mass loss.

As seen from Fig. 1, rotating clusters tend to have smaller concentration: for models with $W_0 = 6$, r_t/r_c decreases from 18 for $\omega_0 = 0$ to 9.6 for $\omega_0 = 0.6$. It is well known that the time to core-collapse in units of $\tau_{rh,i}$ decreases with increasing r_t/r_c for isolated models, but we find the opposite trend for rotating models. Clearly, rotation plays an important role in accelerating the core-collapse.

In Fig. 5, we display the time to core-collapse, in units of initial relaxation times, as a function of initial central concentration for non-rotating King models ($W_0 = 3$ or $W_0 = 6$, equivalent to a wide range of initial central concentration $c = \log(r_t/r_c)$). In particular we examine here the difference between isolated and tidally limited models. For isolated models, $t_{cc}/\tau_{rh,i}$ decreases monotonically with

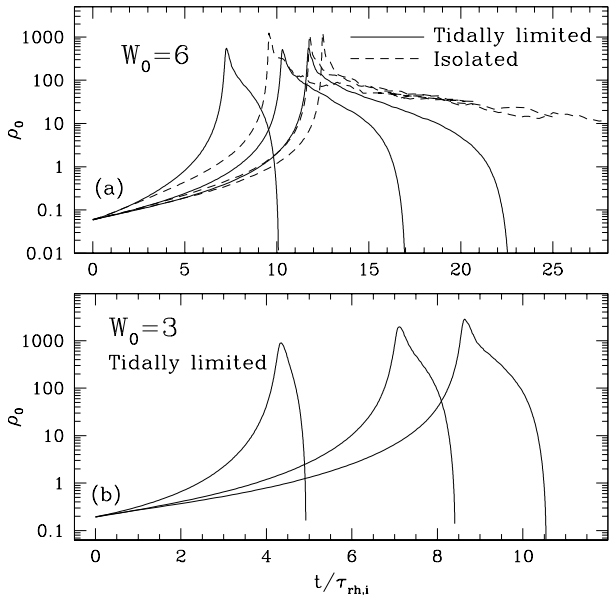

Figure 3. Comparison of central density evolution for models with $W_0 = 6$ (a), and for models with $W_0 = 3$ (b). The initial degree of rotations are $\omega_0 = 0.6, 0.3, 0.0$ for $W_0 = 6$ and $\omega_0 = 1.5, 0.8, 0.0$ for W_0=3, from left to right. The evolution of central density for models without tidal boundaries also shown (dashed lines in (a)).

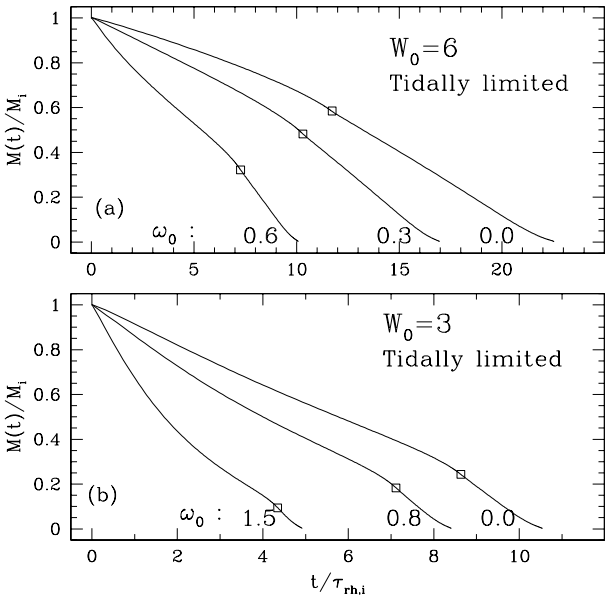

Figure 4. Evolution of total mass retained in the cluster models with $W_0 = 6$ (a), and with $W_0 = 3$ (b). Open squares denote the times for core collapse.

Table 2. Time-scales of tidally limited cluster models.

W_0	ω_0	$t_{cc}/\tau_{rh,i}$	$t_{dis}/\tau_{rh,i}$	$\frac{t_{dis}-t_{cc}}{M_{cc}/\sqrt{G\bar{\rho}}}$	M_{cc}	$t_{50}/\tau_{rh,i}$
	0.0	11.73	22.61	0.119	0.59	13.2
6	0.3	10.31	16.96	0.123	0.48	10.1
	0.6	7.27	10.08	0.144	0.33	5.4
	0.0	8.63	10.54	0.375	0.25	5.4
3	0.8	7.12	8.41	0.405	0.18	4.0
	1.5	4.35	4.92	0.499	0.09	1.7

t_{cc}: core collapse time.
t_{dis}: dissolution time of clusters.
t_{50}: time at which the cluster lose half its total mass.
M_{cc}: represents the mass retained in a cluster at $t \approx t_{cc}$.

increasing c. This behaviour can be compared with the core-collapse times of isolated clusters with fixed $W_0 = 6$ but different ω_0. Contrary to the fact that the non-rotating isolated models have longer $t_{cc}/\tau_{rh,i}$ for less concentrated initial models, the rotating models show an opposite trend. The rotation obviously is fully responsible for the acceleration of the isolated models.

For the tidally limited models, the behaviour of t_{cc} as a function of initial c is not monotonic anymore because of the role of mass loss. Initially less concentrated models lose a significant fraction of their mass by the time of core collapse, and thus the $t_{cc}/\tau_{rh,i}$ becomes smaller for for smaller c starting at around $c \approx 1.1$ (just below $W_0 = 6$). Therefore, we can understand the further reduction of the core-collapse times for tidally limited models as the action of the mass loss.

The post-collapse evolution of *isolated* rotating and non-rotating systems becomes very similar after about $t/\tau_{rh,i} > 15$ (dashed curves in upper panel of Fig. 3). The similarity of post collapse evolution of initially different models at later times can be understood in terms of simple energy balance arguments. Goodman (1987) and Lee (1987) showed that the central density during the post-collapse evolution follows $(t-t_{cc})^{-2}$ if the major driving energy source is three-body binaries. The amplitude is mainly determined by the density at maximum collapse, which is nearly the same for different ω_0 for a fixed W_0 in the models shown in Fig. 3. At later times the difference in t_{cc} does not play an important role, and the evolution becomes similar to each other. The core-collapse can be accelerated by the rotation, but the post-collapse evolution, which is mostly determined by the energy balance between the central heating and the overall expansion, is not sensitive to the presence of the rotation for the *isolated clusters*.

In the presence of a tidal cutoff, however, the simple energy argument does not provide power law behaviours of cluster parameters (Lee, Fahlman & Richer 1991) because of the mass loss. The rate of mass loss becomes an important factor in determining the course of post-collapse evolution. Lee & Ostriker (1987) showed that the lifetime of the clusters in steady tidal field is approximately proportional to $N/\sqrt{G\bar{\rho}}$, where N is the number of stars and $\bar{\rho}$ is the mean density, which remains constant throughout the evolution if the tidal field does not depend on time, of the cluster.

We have summarized some important times in units of $\tau_{rh,i}$, as well as the time until the complete disruption from the core collapse, and remaining mass at the time of core

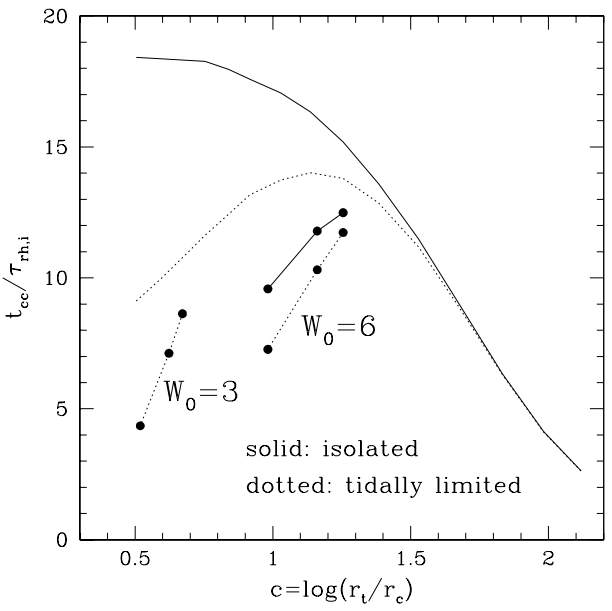

Figure 5. The time to core collapse for non-rotating King models as a function of the initial central concentration $c(=\log(r_t/r_c))$. The core collapse time behaves monotonously with c for isolated models, but not for tidally limited models. We also have shown the collapse times of our rotating models. Note that there is some discrepancy between the results obtained by 1D FP code and FOPAX applied to non-rotating clusters, as seen from Fig. 2.

collapse in Table 2. The time evolution of the total mass of our models is shown in Fig. 4.

3.3 Evaporation Rates

Since $\tau_{rh} \propto \sqrt{N} r_h^{3/2}$ and $t_{dis} \propto N r_t^{3/2}$, disruption time in units of $\tau_{rh,i}$ is proportional to $(r_t/r_h)^{3/2}$. From Table 1, we expect that $t_{dis}/\tau_{rh,i}$ would be reduced by about a factor of 2 from $\omega = 0.6$ to $\omega_0 = 0$, for $W_0 = 6$ models, and by a factor of 1.56 from $\omega_0 = 1.5$ to $\omega_0 = 0$ for $W_0 = 3$ models. The disruption time scales listed in Table 2 for models with different W_0 and ω_0 show somewhat faster evolution of rotating models compared to that of the scaling law above. This may be interpreted as the role of the rotation on the mass loss rate.

The evaporation process can be simply understood as a continuous generation of stars with velocity greater than the escape velocity (v_e) through the dynamical relaxation. For isolated uniform stellar systems, $\langle v_e^2 \rangle = 4\langle v^2 \rangle = 4 v_{rms}^2$ (Ambartsumian 1938; Spitzer 1940), where the brackets denote the mass-weighted average over the cluster. If we assume that an equilibrium velocity distribution $f(v)$ is established in half-mass relaxation time and that the stars are removed uniformly, the dimensionless mass loss rate becomes

$$\xi_e \equiv -\frac{t_{rh}}{M}\frac{dM}{dt} = \frac{\int_{\langle v_e^2 \rangle^{1/2}}^{\infty} f(v) d^3\mathbf{v}}{\int_0^{\infty} f(v) d^3\mathbf{v}}. \quad (2)$$

By employing $\langle v_e^2 \rangle^{1/2} = 2 v_{\rm rms}$ and assuming Maxwellian velocity distribution, Ambartsumian (1938) and Spitzer (1940) obtained $\xi_e = 0.00738$. For tidally limited models, the escape energy is reduced by GM/r_t from the simple estimate given above since the stars are evaporated when they have enough energy to leave tidal boundary. By assuming $W = -0.4GM^2/r_h$, the escape velocity can be expressed as (Spitzer 1987, §3.2)

$$\langle v_e^2 \rangle^{1/2} = 2\,(1-\lambda)^{1/2}\ \ \langle v^2 \rangle^{1/2}, \quad (3)$$

where

$$\lambda = \frac{GM}{r_t} \,/\, \frac{0.8GM}{r_h} = \frac{5 r_h}{4 r_t}. \quad (4)$$

We denote the evaporation rate obtained by using reduced escape velocity as Ambartsumian-Spitzer (abbreviated as AS) rate ($\xi_{\rm AS}$).

In Fig. 6, we have shown the behavior of ξ_e of our models with $W_0 = 6$ together with $\xi_{\rm AS}$ using r_h/r_t data from the evolving models. The actual ξ_e is usually larger than $\xi_{\rm AS}$ by a factor of 2 or more. The Ambartsumian-Spitzer formula assumes that the stellar evaporation takes uniformly over the cluster. This is clearly a very simplified assumption, and could be the reason for the discrepancy. Such discrepancies are also noticed by Takahashi & Lee (2000). We simply note that the general tendency is similar between the model and AS formula. As we will see below, large fraction of angular momentum is removed by the time of post-collapse phase. However, the effect of rotation seems to be persistent on the stellar evaporation rate, although the effect is much smaller than during the pre-collapse. During the post-collapse phase, there exists differences among ξ_e with different initial rotation parameters. This might be an indication of the importance of the rotation on the stellar evaporation. Although the angular momentum disappears rather quickly as the cluster loses mass, the location of the maximum rotation moves outward so that the rotation plays some role in mass evaporation. (see below)

3.4 Angular Momentum Transport

Two-body relaxation causes the angular momentum to diffuse outward. The stars with high angular momentum preferentially move outward and eventually escape from the cluster. Therefore, the angular momentum decreases with time. In Fig. 7, we have displayed the evolution of rotational energy in units of total energy for our models. The epochs of core collapse are indicated as squares in the figure. By the time of core collapse, the rotational energy becomes only a very small fraction of total energy, and the loss of rotational energy is even accelerated during the post-collapse phase.

Evolution of the rotational speed along the equator can be followed in several ways. Fig. 8(a) displays the time evolution of rotational speed at half-mass and core radii of the initial models in equator for models with tidal boundary. The rotation speed at initial half-mass radii for both models with different initial degrees of rotation (ω_0= 0.3, 0.6) decrease monotonically with time. However, evolution of rotation speed at a radius of initial core radius shows a different structure, especially for the model with initial degree of rotation of $\omega_0 = 0.6$. The rotation speed at a radius of initial core radius shows a slight increase during $t/\tau_{rh,i} \leq 2$. Inside the core the rotation structure can be approximated as a rigid body. Hachisu (1979) claimed that a stellar system

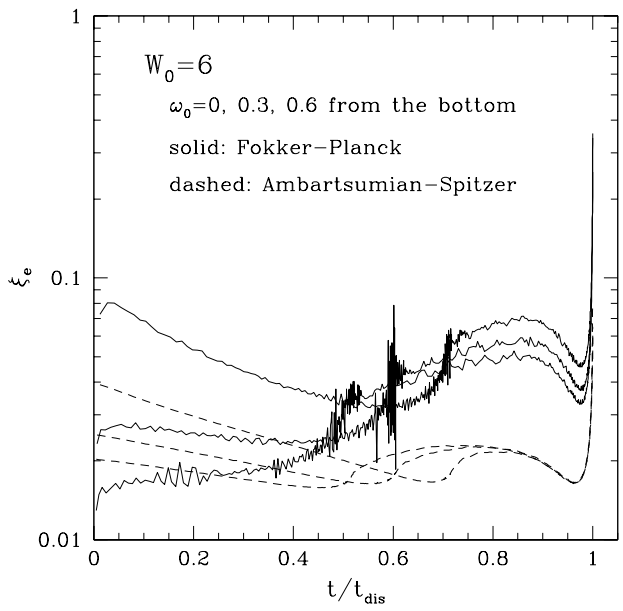

Figure 6. The mass ejection rate computed from our Fokker-Planck models (solid line) and from Ambartsumian-Spitzer formula, for $W_0 = 6$ models (dashed line). The noise in estimates of ξ_e near the collapse is mainly due to the fact that we have kept only three decimal points in mass estimates while the time step becomes very small during these phases.

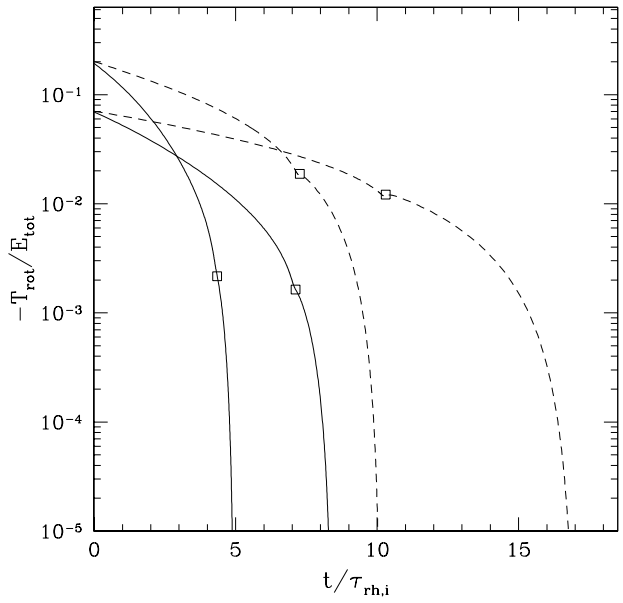

Figure 7. Evolutions of rotational energy in units of total cluster energy for $W_0 = 3$ (solid lines) and $W_0 = 6$(dashed lines). The epochs of maximum collapse are indicated as open squares.

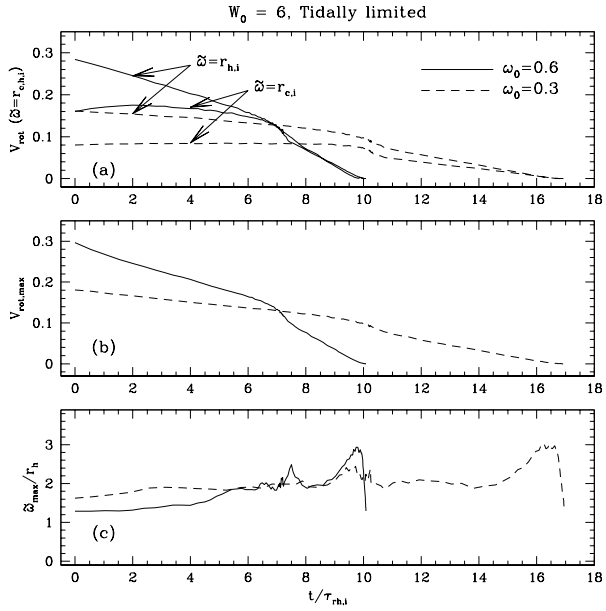

Figure 8. Evolutions of rotational velocity for models with $W_0 = 6$ and $\omega_0 = 0.6$(solid lines) and $\omega_0 = 0.3$(dashed lines). The time evolution of rotational velocity for two fixed radii of the initial core and half-mass radii is shown (a). Mid panel (b) shows time evolution of the maximum value of rotational velocity at the equator. The ratio between the radius where the rotational velocity is maximum in equator and the half-mass radius is displayed in lower panel (c).

with constant angular velocity should experience gravo-gyro catastrophe owing to a negative specific moment of inertia. Near the initial core radius, the rotation speed increases due to the negative specific moment of inertia.

Some amount of rotation is still present after core bounce as shown in Fig. 8(b), which displays evolutions of maximum rotation speed $V_{rot,\max}$ in the equator. The maximum rotation speed decreases monotonically throughout entire evolutionary stage. The rotation speed decreases rather rapidly after the core collapse. The ratio between half-mass radius and the radius in equator where the rotation speed has a maximum value is shown in Fig. 8(c) for tidally limited models. The model with strong rotation has a value around ~ 1.4 until $t/\tau_{rh,i} \leq 3$, then increases gradually until the collapse. The global value of this ratio is around 2 irrespective of initial degrees of rotation.

Fig. 9 shows the time evolution of z-component of specific angular momentum which is defined by,

$$J_z(\tilde{\omega}) = v_{\rm rot}(\tilde{\omega})\tilde{\omega}. \quad (5)$$

Fig. 9(a) shows that the angular momentum at $r = r_{h,i}$ decreases faster than the J_z at $r = r_{c,i}$, where $r_{h,i}$ and $r_{c,i}$ are initial half-mass and core radii, respectively, with initial rotation parameter $\omega_0 = 0.6$. A similar pattern is shown for the model with slower initial rotation, but not clearly. Fig. 9(b) displays the time evolution of maximum angular momentum in the equator. The location of $J_{z,max}$ in units of r_h is shown in the lower panel of Fig. 9. It clearly shows the outward movement of angular momentum.

The rotation curves at selected epochs are shown in Fig.

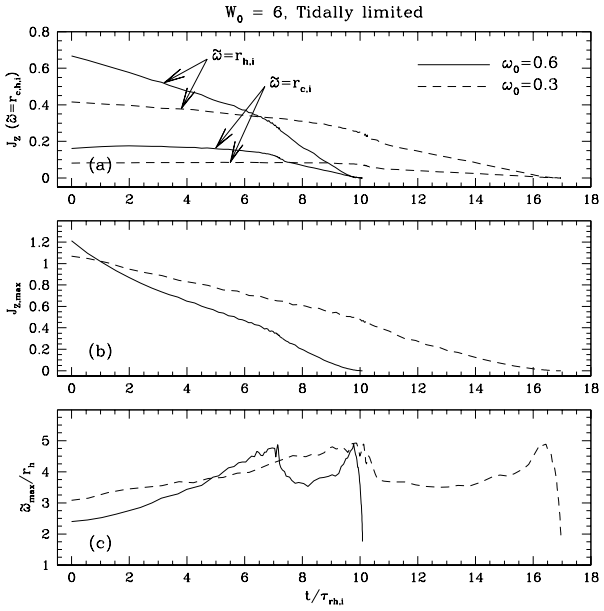

Figure 9. Same as Fig. 8, but for z-component of angular momentum (see equation (5) for definition).

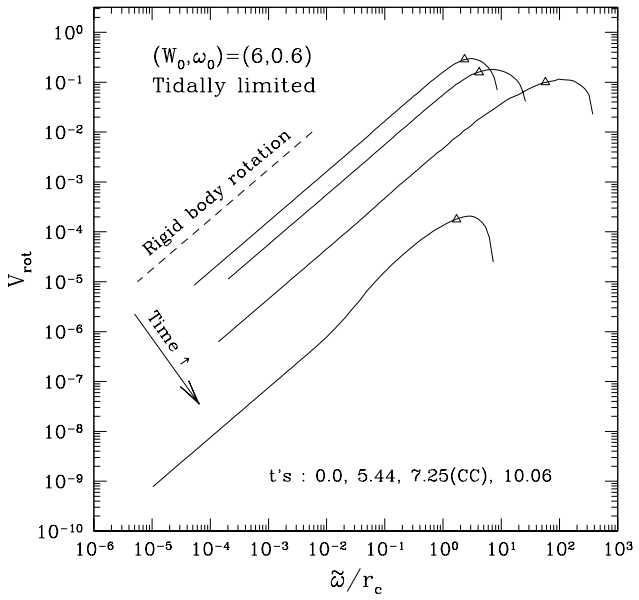

Figure 10. Radial profiles of rotational velocity in equator for tidally limited cluster model $(W_0, \omega_0) = (6, 0.6)$ at four different evolutionary stages. For comparison, the rotation profile for solid body is shown (dashed line). The mass retained in a cluster is about a half of initial mass at $t/\tau_{rh,i} = 5.44$. At $t/\tau_{rh,i} = 10.06$ the cluster is dissolved. Half-mass radii are marked with open triangles. Note that the radius is measured in unit of current core radius.

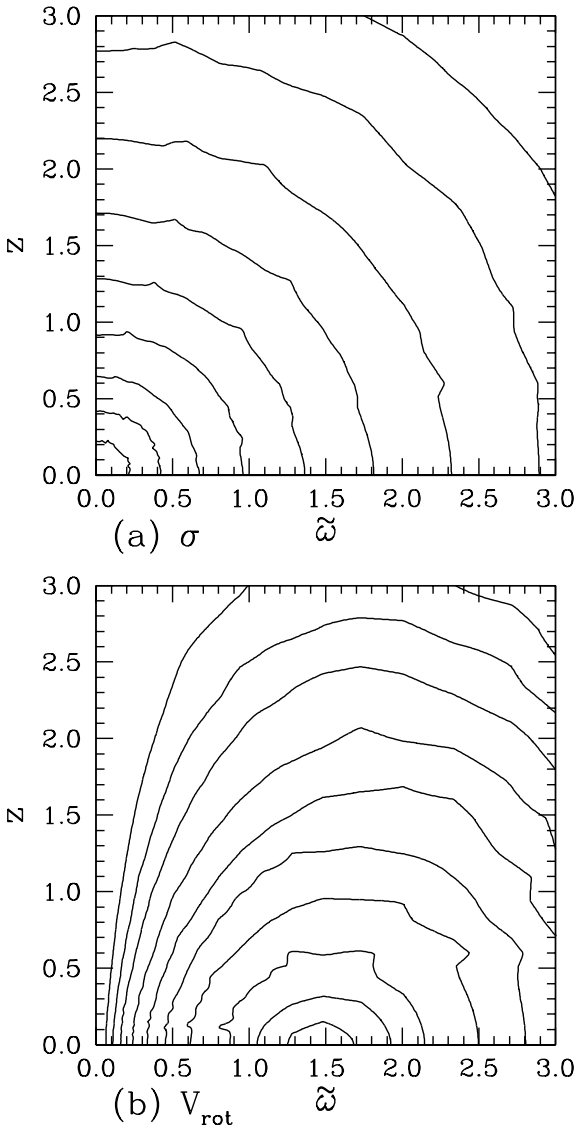

Figure 11. Two dimensional structure of cluster model in the meridional plane with $(W_0, \omega_0) = (6, 0.6)$ and with tidal boundary at $t/\tau_{rh,i} = 9.03$. One dimensional velocity dispersion (a) and rotational velocity (b) are shown.

10 for $(W_0, \omega_0) = (6, 0.6)$. Because of angular momentum loss, the rotation speed tends to decrease with time, but the shape of the curve remains nearly the same. The angular speed is nearly constant (i.e., rigid body rotation) up to r_h, and drops rapidly toward the tidal radius.

The 2-dimensional structure of cluster with $(W_0, \omega_0) = (6, 0.6)$ with tidal boundary in the meridional plane is shown in Fig. 11 at a time $t/\tau_{rh,i} = 9.03$. Note that the axes are measured in units of initial core radius and that the current core and half-mass radii have already decreased to $\sim 0.038 r_{c,i}$ and $\sim 0.64 r_{c,i}$, respectively. The one-dimensional velocity dispersion shows a clear sign of collapsed core, i.e., linearly increasing velocity dispersion toward cluster center. The morphology of two-dimensional rotational velocity after

core bounce shows a similar structure to that of pre-collapse phase (see Paper I for comparison), although the degree of rotation decreased.

3.5 Velocity Dispersion and Angular Speed

In Fig. 12, we have shown the time evolution of central velocity dispersion (σ_0) and central rotational angular speed (Ω_0). As we have seen from the rotational curves in Fig. 10, the central parts have the rigid body rotation, and the angular speed is a constant out to large radius.

Both σ_0 and Ω_0 increase with time rather slowly until core collapse and decrease afterward. The increase of Ω_0 is a consequence of the gravo-gyro instability. During the post-collapse, these quantities drops rapidly with time. The general behavior of σ_0 does not seem to be affected by the presence of rotation. As we will see in §3.7, rotation energy is only a small fraction of the total kinetic energy near the center throughout the evolution.

The relationship between the central density and σ_0, and Ω_0 are shown in Fig. 13. For σ_0 versus ρ_0, we have plotted all six models of Table 1, while only rotating four models are shown for Ω_0 versus ρ_0 figure. The velocity dispersion is nearly independent of initial rotation: all models with the same W_0 fall on nearly single lines. The power-law behavior of σ_0 on ρ_0 during the pre collapse phase is a consequence of self-similarity of collapsing core. During this phase, it is well known that $\sigma_0 \propto \rho_0^{0.1}$ (e.g., Cohn 1980). During the post-collapse phase, we can again apply the energy balance argument to obtain $\sigma_0 \propto \rho_0^{1/6} M^{1/9}$. For isolated clusters, $M = constant$ and $\sigma_0 \propto \rho_0^{1/6}$. Since both M and ρ_0 decrease with time, we expect that $\beta > 1/6$ if we express $\sigma_0 \propto \rho_0^{\beta}$. Our result in Fig. 13 shows that $\beta \approx 0.23$.

The angular speed also appears to follow power law on ρ_0 during the pre collapse phase, except for the early stage of evolution for models with central potential of $W_0 = 3$. Although the behavior of Ω_0 during the post-collapse phase depends on the amount of angular momentum loss by the end of the core-collapse, it still has a power-law relation with central density, ρ_0.

3.6 Core and Half-mass Radii

The evolution of r_c/r_h for models with central potential of $W_0 = 6$ is shown in Fig. 14: the upper panel is for the tidally limited clusters and the lower panel is for isolated clusters. For tidally limited clusters, more rapidly rotating initial models show larger value of r_c/r_h due to smaller r_h than slowly rotating models. Both r_c and r_h decrease with time although there is a difference in decreasing rate depending on the initial degree of rotation. For example, r_c/r_h remains nearly constant in the early phase for our $\omega_0 = 0.6$ model, while other models show gradual decrease. After core bounce, both r_c and r_h increase, but r_c increases more rapidly than r_h. In the late phase of the evolution r_h decreases again due to a large amount of mass loss. The minimum values of r_c/r_h are nearly independent of ω_0.

For isolated clusters, all models show similar value of $r_c/r_h \sim 0.007$ after core bounce. Again, this is due to the fact that the cluster remains self-similar if the post-collapse is dominated by three-body binary heating. According to

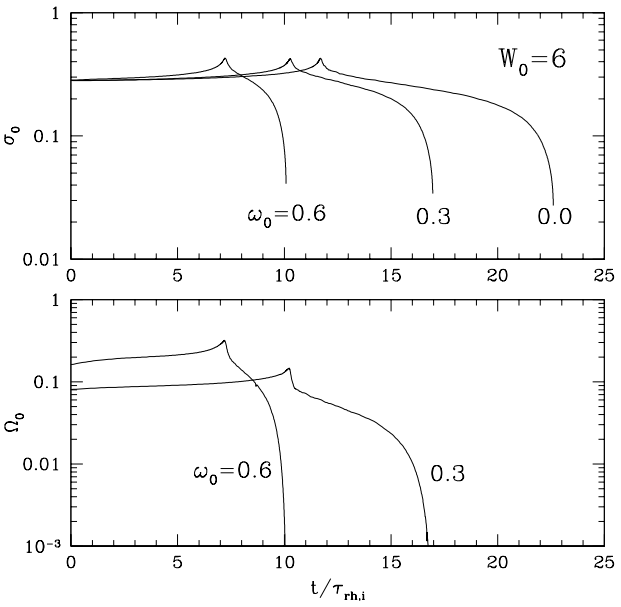

Figure 12. Time evolution of central velocity dispersion and central angular speed for models with $W_0 = 6$ and $\omega_0 = 0.0$, 0.3 and 0.6.

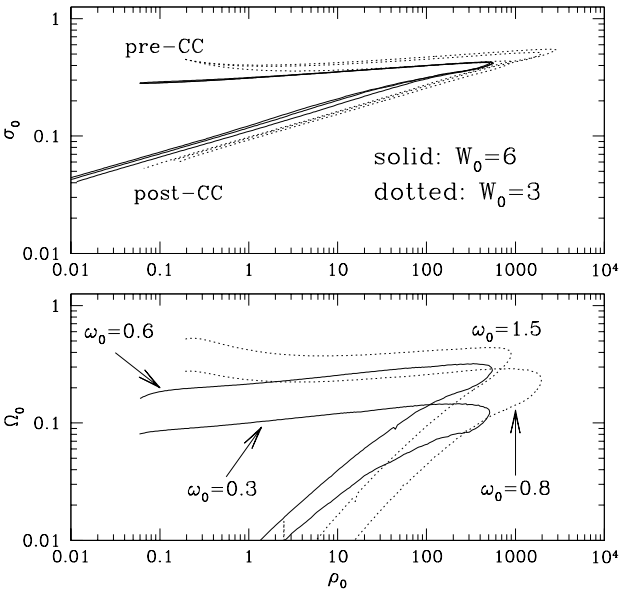

Figure 13. The evolution of σ_0 and Ω_0 as a function of ρ_0 for all six models shown in Table 1. The velocity dispersion follows power-laws during pre and post collapse phase, and is nearly independent of rotation. The angular speed also follows near power-law on ρ_0 during the collapsing phase.

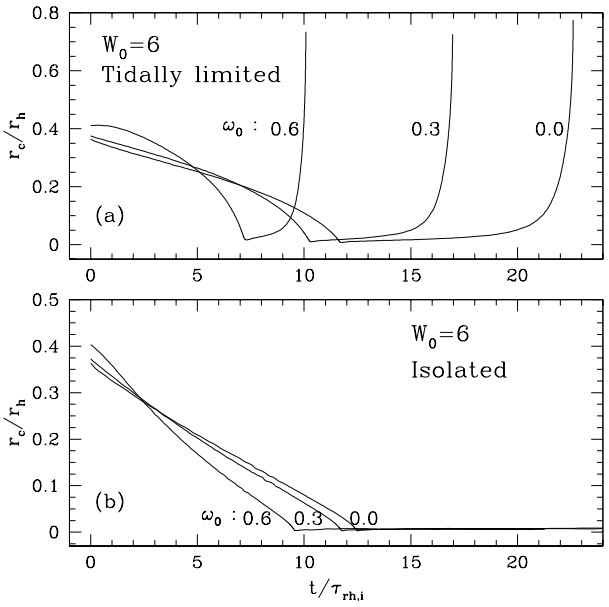

Figure 14. Ratio between core and half-mass radii for models with tidal boundary (a) and for models without tidal boundary (b). The central potential for both models is $W_0 = 6$.

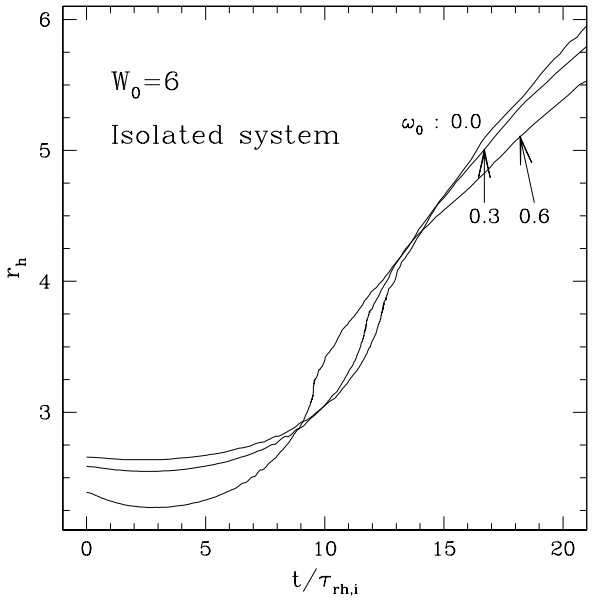

Figure 15. Comparison of half-mass radii for models with $W_0 = 6$, and without tidal boundary. The half-mass radius for model with higher value of initial rotation is seen clearly to be smaller than the half-mass radii for models slower/no initial rotations.

the self-similar model by Goodman (1987), $r_c/r_h \propto N^{-2/3}$, and thus it should be factor of ~ 1.84 smaller than the case with $N = 2000$: we find that our value is about a factor of 2 smaller than the N-body calculation by Giersz & Heggie (1994b) with $N = 2000$.

Since our system is axisymmetric, it is a little bit difficult to define the half-mass radius. We used the same definition as in Paper I. For early stages of the evolution, when the system is more flattened, the method used here (and also in Paper I) may be problematic though the difference is small. However, after core bounce we expect that the difference between true half-mass radius and the half-mass radius computed in the present study is negligible.

The evolution of r_c/r_h depends sensitively on the choice of boundary conditions. Strong increase of r_c/r_h after core bounce for tidally limited clusters is mainly due to strong mass loss. The effect of rotation after core bounce is shown in Fig. 15, which displays the evolution of r_h for isolated clusters with initial central potential of $W_0 = 6$. After core bounce, r_h for initially rapidly rotating cluster ($\omega_0 = 0.6$) increases more slowly than the model without initial rotation. The difference of r_h between two models is ~ 6 % at $t/\tau_{rh,i} \sim 20$. Although we tried to keep these stellar systems isolated from any tidal effect, there is some amount of mass loss through the computational boundary. The amount of mass loss for our isolated models is ~ 2 percent, irrespective of initial degrees of rotation at the end of our calculation. Therefore, we conclude that the difference between half-mass radii (in late evolutionary stages) for different initial rotation for isolated models is due to rotation, which is still present near a radius of $r \sim r_h$. The smaller value of r_h for a more rapidly rotating cluster can be explained by a transfer of z-component of angular momentum(J_z) in outward direction. So, in contrast to our findings (for the isolated cluster only) that the post-collapse core structure, as represented by Cohn's dimensionless central potential, does not depend on initial rotation, we find here that at the half-mass radius the system still remembers about its different initial degrees of rotation.

3.7 V_{rot}/σ

We try to give some evidence what could be the consequences of our model simulations for the interpretation of velocities (rotational and dispersion) in globular star clusters. It has to be emphasized, however, that due to the idealized nature of our numerical studies (e.g. equal point masses, no tides, no stellar evolution) such discussion must be preliminary and can certainly not be done on a quantitative, but rather on a more qualitative level.

V_{rot}/σ has been analyzed in our model clusters, where V_{rot} denotes the rotational velocity, and σ the 1D velocity dispersion, as a function of time and radius. V_{rot}/σ describes the relative importance of rotational versus pressure support in the local cluster kinematics and dynamics; while it has been very successfully used in observational studies of elliptical galaxies and bulges of spiral galaxies this quantity recently has become available also from globular cluster observations (Gebhardt 2001, personal communication).

In Fig. 16, we have shown the runs of V_{rot}/σ as a function of radius in units of half-mass radius for the model

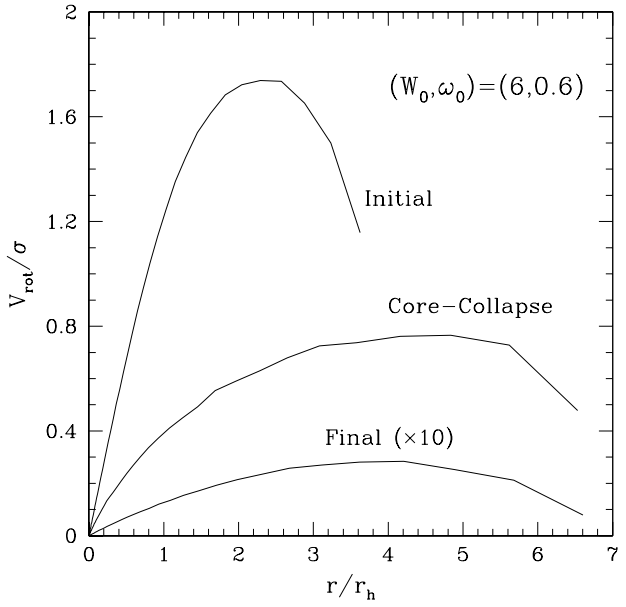

Figure 16. V/σ as a function of radius in units of half-mass radius for models with initial $W_0 = 6$, and $\omega_0 = 0.6$ at three epochs as indicated in the figure. The location of maximum V_{rot}/σ moves outward.

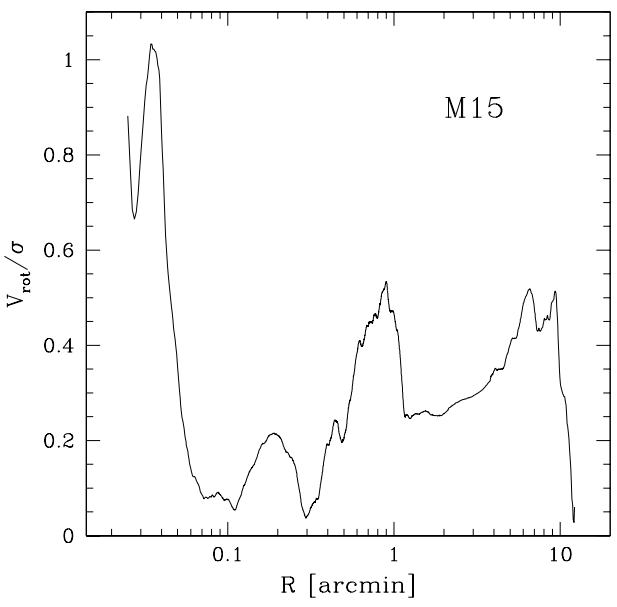

Figure 17. V_{rot}/σ as a function of radius in arc minutes for M15 (data provided by Gebhardt).

with initial $W_0 = 6$ and $\omega_0 = 0.6$ at three epochs: initial model, at core-collapse, and near final disintegration. We notice from this figure that the position of the maximum V_{rot}/σ relative to r_h moves outwards with time. This is another indication of angular momentum transport. Also note that $(V_{rot}/\sigma)_{\max}$ for the initial model is much larger than the late values of an evolved cluster, it decreases monotonically with time. For this particular model, the $(V_{rot}/\sigma)_{\max}$ becomes around 0.8 at the core collapse, and further decreases in the post-collapse phase to very small values smaller than 0.1. Towards the centre the models presented in this paper all show a decrease of (V_{rot}/σ) to zero. This is consistent with what we see in Fig. 10, that the stars rotate like solid body roughly inside half-mass radius, regardless of the the evolutionary phase. Note that we obtained V_{rot} and σ in the rotational plane, and the observed value of V_{rot}/σ should be always be smaller than this figure.

Gebhardt (personal communication) provides some new data on direct measurements of V_{rot}/σ in M15, which are shown in Fig, 17. Regarding the outer zones of the cluster, our data are consistent with one of our post-collapse models starting at $W_0 = 6$ and $\omega_0 = 0.6$, i.e., an initially fairly large amount of rotation, as far as the core, half-mass and outer radii are considered. But for the central regions he finds a strong rise in the observed rotational speed, which is not present in our models. Note, however, that multi-mass models obtained with an earlier version of our code offer a possible explanation for this phenomenon: the gravo-gyro instability effect (Hachisu 1979) is much more pronounced if a mass spectrum is present as compared to the equal mass model (see for that Fig. 4 of Paper 1). Heavy masses go into core bounce with a strong acceleration of rotational velocity and a decrease of dispersion velocity, so they would exhibit a high V_{rot}/σ in the centre (compare figure in Spurzem & Einsel 1998, where the angular velocity and the dispersion velocity of ten mass components in the centre are shown as a function of time). We will further study this effect in future work.

Though many of the Galactic globular clusters do not rotate significantly, there have been rotation curves measured for some clusters earlier (Meylan & Mayor 1986; Lupton et al. 1987; Gebhardt et al 1994, 1995). The clusters with measured rotation includes ω Cen, 47 Tuc, M13, M15, and NGC6397. For most of these clusters, the rotation measurements are done in a rather limited range and rotation curves are hardly known. Also in earlier papers, Gebhardt et al. (1995) made very careful measurements of stellar velocity field using Fabry-Perot spectrophotometer and found that the projected rotation velocity rises or remains nearly flat from $30''$ to $10''$ for M15, 47 Tuc, and NGC 6397. As was discussed above this cannot be reproduced in our equal mass models here yet, but we think a multi-mass model could be able to explain the effect. Also in the case of 47 Tuc the rotation curve seems to be consistent with the solid body rotation up to $\sim 2'$ corresponding to $\sim 0.7 r_h$, although again the very central part appears to deviate from the solid body rotation.

We need density and velocity dispersion profiles as well as the rotation curve in order to estimate the relative rotational energy (such as $-T_{rot}/E_{tot}$). Assuming same V_{rot}/σ throughout the cluster, we estimate $-T_{rot}/E_{tot} = 0.013 \sim 0.05$. The dynamical ellipticities expected lie in the range of 0.03 to 0.05, depending on the inclination. The observed ellipticities of these clusters are roughly consistent with the V_{rot}/σ, although there are large uncertainties on the estimates of ellipticities.

4 CONCLUSION

The first self-consistent evolutionary models of rotating star clusters in the post core collapse phase have been obtained by improving an earlier version of a FOPAX for axially symmetric systems. For that purpose the code used in previous models of pre-collapse rotating clusters (Einsel & Spurzem 1999, Paper I) has been improved by including a three-body binary heating and also in some of its numerical procedures. We start as initial models with generalized King models including rotation and study a few fiducial cases with dimensionless central potential W_0 3 or 6, and a dimensionless rotation parameter ω_0 from 0.0 (no rotation, spherical system) to 1.5 for $W_0 = 3$ and 0.0 to 0.6 for $W_0 = 6$. While most of the model star clusters include a tidal boundary modelled by an energy cutoff, we discuss one sequence of isolated models ($W_0 = 6$) to distinguish the effects of internal relaxation and tidally induced mass loss.

Our results show that, as in the pre-collapse case (compare with Paper I), the evolution of the tidally limited cluster is significantly accelerated by initial rotation. Comparing with isolated models we find that in pre-collapse the acceleration of evolution is due to a combination of both internal relaxation (enhanced by the increased fraction of ordered motion in the system) and easier escape across the tidal boundary in the co-rotating direction. For post-collapse however, the isolated systems do not show any strong dependence of their structure and evolution due to initial rotation. However, in case a tidal field is present, the rotating cluster starts off into the post-collapse phase with a slightly larger ratio of core over half-mass radius r_c/r_h, and a slightly shallower value of the central potential, and this triggers a faster evolution during its complete lifetime, up to the final dissolution. The acceleration of its evolution is comparable to that found in the pre-collapse state in Paper I.

Evidently, models with higher initial rotation dissolve faster in the tidal field. The effect of rotation disappears after $t/\tau_{rh,i} \sim 3$ for model with initial rotation of $\omega_0 = 0.6$. The mass loss rate after core collapse is different from each other depending on initial degrees of rotation. However, the main reason for the difference of mass loss rate is a shallower scaled central potential for highly rotating model at a time of core collapse than the model without initial rotation. Therefore we conclude that the overall shape of cluster changes very little after core collapse irrespective of initial degrees of rotation.

The rotational energy decreases all the time as the cluster loses mass, together with angular momentum. By the time of core collapse, the rotational energy becomes some fraction of its initial value. But still initially rotating and non-rotating clusters exhibit different structure properties at intermediate radii, e.g. in their ratio r_c/r_h, and the (V_{rot}/σ) value (rotational velocity over 1D velocity dispersion) has a clear maximum as a function of radius, and the radial position of this maximum (measured in units of the half-mass radius) goes out. The maximum value of (V_{rot}/σ) at a given time decreases monotonically with the dynamical age of the cluster, even across core collapse. We stress that this is a possible unambiguous dynamical clock to measure dynamical ages of clusters, which is not reset to zero as the cluster undergoes core bounce and re-expansion. Its present value allows also to put certain limits on the initial amount of rotational energy in clusters. Our values of (V_{rot}/σ) can be confronted with much improved recent observations of rotation curves in globular clusters (Gebhardt 2001, personal communication). We can pinpoint a post-collapse evolutionary state where our model cluster has a maximum value $(V_{rot}/\sigma)_{\max}$ which matches the observed value, e.g., in M15; on the other hand our present models do not reproduce the observed strong increase in central rotation, we rather have always a rigid body rotation in the central regions; but preliminary multi-mass models (Spurzem & Einsel 1998) are indeed able to explain the observed effect. It is a strongly pronounced occurrence of what was found by Hachisu (1979) as gravo-gyro catastrophe; it is much less pronounced in the equal mass system, but the heavy masses in a multi-component system are strongly subject to it (Spurzem & Einsel 1998).

Most of the results discussed in this paper, however, are still derived from an equal mass model. Actual clusters should have a mass spectrum, and the observed rotation curves are usually dominated by the brightest component. In order to compare with the observed clusters, we need to further study the multi-mass models rather than equal-mass models. Also, we treat the cluster as a 2D model in phase space only (distribution function $f = f(E, J_z)$ only depends on two constants of motion, energy, and z component of angular momentum). So all relaxation effects (diffusion coefficients) do not discriminate between different orbits having same E and J_z, but different third integral I_3. In Paper I some discussion of the possible errors is given by measuring the artificial flattening of an initially spherical system treated by our axisymmetric model. Here we do not continue this, but propose for the near future an extensive study of direct N-body models of rotating clusters, similar in scope to the seminal results obtained for non-rotating clusters by Giersz & Heggie (1994a, 1994b, 1996). This will make it possible to assess the validity of our approximations. Preliminary studies of a few of such models do exist (Boily 2000, Boily & Spurzem 2000) and they support the Fokker-Planck results, but they do by any means not provide a broad enough statistical and parameter range.

Acknowledgments

We are grateful to generous support from BK21 program. This work was partially supported by the interdisciplinary grant from Seoul National University. R.Sp. wants to thank the Dept. of Astronomy, Seoul National Univ., and in particular H.M. Lee, E. Kim, and many other colleagues there for generous and very friendly hospitality during a research visit in Korea. Part of this work has been completed during a research stay at the Univ. of Tokyo under the collaborative German-Japanese research grant DFG/JSPS 446 JAP-113/18/0-2. R.Sp. thanks the colleagues at Univ. of Tokyo for friendly and supportive hospitality. E.K. & M.G.L. are supported in part by the MOST/KISTEP international collaboration research (1-99-009).

REFERENCES

Aarseth S.J., 1985, in Brackbill J.U., Cohen B.I., eds, Multiple time scales, Academic Press, Orlando, p. 378

Aarseth S.J., 1996, in Hut P., Makino J., eds, Dynamics of Star Clusters, Proc. IAU Symp. No. 174, p. 161

Aarseth S.J., 1999a, PASP, 111, 1333

Aarseth S.J., 1999b, CeMDA, 73, 127

Aarseth S.J., Heggie D.C., 1998, MNRAS, 297, 794

Agekian T.A., 1958, Soviet Astronomy AJ, 2, 22

Ambartsumian, V. A., 1938, *Ann. Leningrad State U.*, No. 22 [translated in Proc. IAU Symp. No.113, Dordrecht, Reidel (1985)]

Baumgardt H., 2001, MNRAS, in press (astro-ph/0012330)

Bettwieser E., Sugimoto D., 1984, MNRAS, 208, 493

Boily, C.M., 2000, Lan con A., Boily C.M., eds, Massive Stellar Clusters, ASP Conf. Ser. No. 211, ASP: San Francisco, p. 190

Boily, C.M., Spurzem R., 2000, in Noels A., Magain P., Caro D., Jehin E., Parmentier G., & Thoul A.A., eds, The Galactic Halo : From Globular Cluster to Field Stars, Proc. of the 35th Liège Intern. Astroph. Colloq. p. 607.

Cohn H., 1979, ApJ, 234, 1036

Cohn H., 1980, ApJ, 242, 765

Deiters S., Fuchs B., Just A., Spurzem R., Wielen R. (eds.), 2001, Dynamics of Star Clusters and the Milky Way, ASP Conf. Ser. No. 228, ASP: San Francisco

Einsel C., Spurzem R., 1999, MNRAS, 302, 81 (paper I)

Gao, B., Goodman, J., Cohn, H., Murphy, B., 1991, ApJ, 370, 567

Gebhardt, K., Pryor, C., Williams, T. B., & Hesser, J. E., 1995, AJ,108, 2067

Gebhardt, K., Pryor, C., Williams, T. B., & Hesser, J. E., 1995, AJ,110, 1699

Giersz M., 1996, in Hut P, Makino J., eds, Proc. IAU Symp, 174, Dynamical Evolution of Star Clusters - Confrontation of Theory and Observations, Kluwer, Dordrecht, p. 101

Giersz M., 1998, MNRAS, 298, 1239

Giersz M., 2001, MNRAS, 324, 218

Giersz M., Heggie D.C., 1994a, MNRAS, 268, 257

Giersz M., Heggie D.C., 1994b, MNRAS, 270, 298

Giersz M., Heggie D.C., 1997, MNRAS, 286, 709

Giersz M., Spurzem R., 1994, MNRAS, 269, 241

Giersz M., Spurzem R., 2000, MNRAS, 317, 581

Gnedin O.Y., Lee, H.M., Ostriker, J.P., 1999, ApJ, 522, 935

Goodman J., 1983, Ph.D. Thesis, Princeton University

Goodman J., 1987, ApJ, 313, 576

Goodman J., Hut, P., 1993, ApJ, 403, 271 1999, AJ, 117, 167

Hachisu I., 1979, PASJ, 31, 523

Heggie D.C., 1984, MNRAS, 206, 179

Heggie D.C., 2001, in Makino J., Hut P., eds, 2001, Astrophysical Supercomputing using Particle Simulations, IAU Symposium No. 208, held 10-13 July 2001 in Tokyo, Japan. ASP Conf. Ser., ASP: San Francisco.

Heggie D.C., Giersz M., Spurzem R., Takahashi K., 1998, in J. Andersen, ed, Highlights of Astronomy Vol. 11, Kluwer Acad. Publishers, 11B, 591

Hurley J.R., Tout C.A., Aarseth S.J., Pols O.R., 2001, MNRAS, in press (astro-ph/0012113)

Hut P., 1985, in Goodman J., Hut P., eds, Proc. IAU Symp. 113, Dynamics of Star Clusters, Reidel, Dordrecht, p. 231

Ibata R.A., Richer H.M., Fahlman G.G., Bolte M., Bond H.E., Hesser J.E., Pryor C., Stetson P., 1999, ApJS, 120, 265

Joshi K.J., Nave C.P., Rasio F.A., 2001, ApJ, 550, 691

Joshi K.J., Rasio F.A., Portegies Zwart S., 2000, ApJ, 540, 969

Lecar M., & Cruz-González C., 1972, in Lecar M., ed, The Gravitational N-Body Problem, Proc. IAU Coll. No. 10, Reidel, Dordrecht.

Lee H.M., 1987, ApJ, 319, 772

Lee H.M., Ostriker J.P., 1987, ApJ, 322, L123

Lee H.M., Fahlman, G., Richer, H., 1991, ApJ, 366, 455

Louis P.D, Spurzem R., 1991, MNRAS, 251, 408

Lupton R.H., Gunn J.E., 1987, AJ, 93, 1106

Lupton R.H., Gunn J.E., Griffin R.F., 1987, AJ, 93, 1114

Lynden-Bell D., 2001, in Deiters S., Fuchs B., Just A., Spurzem R., Wielen R., eds, Dynamics of Star Clusters and the Milky Way, ASP Conf. Ser. Vol. 228, ASP: San Francisco, p. 99.

Makino J., 1996, ApJ, 471, 796 Dynamics of Star Clusters and the Milky Way, ASP Conf. Ser. Vol. 228, 2001, p. 87.

Makino J., Aarseth S.J., 1992, PASJ, 44, 141

Makino J., Hut P., eds, 2001, Astrophysical Supercomputing using Particle Simulations, IAU Symposium No. 208, held 10-13 July 2001 in Tokyo, Japan. ASP Conf. Ser., ASP: San Francisco, in prep.

Meylan, G., Mayor, M., 1986, A&A, 166, 122

Ostriker, J. P., & Peebles, P. J. E., 1973, ApJ, 186, 467

Portegies Zwart S.F., Takahashi K., 1999, CeMDA, 73, 179

Portegies Zwart S.F., Makino J. McMillan S.L.W., Hut P., 1999, A&A, 348, 117

Quinlan G.D., 1996, NewA, 1, 35

Spitzer, L. Jr., 1940, MNRAS, 100, 396

Spitzer, L. Jr., 1987, Dynamical Evolution of Globular Clusters, Princeton Univ. Press

Spurzem R. & Takahashi, K., 2001, in preparation

Spurzem R., 1994, in Pfenniger D., Gurzadyan V.G., eds, Ergodic Concepts in Stellar Dynamics, Springer-Vlg., Berlin, Heidelberg, p. 170

Spurzem R., 1996, in Hut P., Makino J., eds, Dynamics of Star Clusters, Proc. IAU Symp. No. 174, p. 111

Spurzem R., 1999, in Riffert H., Werner K., eds, The Journal of Computational and Applied Mathematics (JCAM), 109, 407, Elsevier Press, Amsterdam.

Spurzem R., 2001, in Deiters S., Fuchs B., Just A., Spurzem R., Wielen R., eds, Dynamics of Star Clusters and the Milky Way, ASP Conf. Ser. Vol. 228, ASP: San Francisco, p. 75.

Spurzem R., Aarseth S.J., 1996, MNRAS, 282, 19

Spurzem R., Baumgardt H., 2001, MNRAS, subm.

Spurzem R., Einsel C., 1998, in D.R. Merritt, M. Valuri, J.A. Sellwood, eds, Massive Stellar Clusters, ASP Conf. Ser. No. 182, ASP: San Francisco, p. 105.

Spurzem R., Takahashi K., 1995, MNRAS, 272, 772

Takahashi K., 1995, PASJ, 47, 561

Takahashi K., 1996, PASJ, 48, 691

Takahashi K., 1997, PASJ, 49, 547

Takahashi K., Lee H.M., Inagaki S., 1997, MNRAS, 292, 331

Takahashi K., Lee H.M., 2000, MNRAS, 316, 671

Takahashi K., Portegies Zwart S.F., 1998, ApJL, 503, L49

Takahashi K., Portegies Zwart S.F., 2000, ApJ, 535, 759